

Experimental Studies on Some Drugs Used in Covid-19 Treatment (Favipiravir and Dexamethasone) in Albino Rats

Moustafa S. Abou El-Fetouh, Nora M. El-Seddawy, Manar A. Abdel Mageed, Mona N. Abd El-Hamed*

Department of Pathology, Faculty of Veterinary Medicine, Zagazig University, Egypt.

*Correspondence

Corresponding author: Mona N. Abd El-Hamed
E-mail address: omona103@gmail.com

Abstract

In this study, the side effects of some anti-covid-19 drugs (Favipiravir and Dexamethasone) were evaluated through the pathological, and clinicopathological changes in the tissues of rats. 30 rats were divided into 6 groups: Gp1- control; Gp2 received 0.54 mg/kg dexamethasone; Gp3 received 200 mg/kg favipiravir; Gp4 received 400 mg/kg favipiravir; Gp5 received 200 mg/kg favipiravir + 0.54 mg/kg dexamethasone, and Gp6 received 400 mg/kg favipiravir + 0.54 mg/kg dexamethasone. Histopathological and clinical results showed that both favipiravir and dexamethasone-induced lesions in the liver, kidney, and lung as well as increased liver functions (alanine transaminase, aspartate aminotransferase, and C-reactive protein) and kidney functions (urea and creatinine). Also increased oxidative stress parameters such as malondialdehyde and decreased antioxidants in liver, and kidney tissues. Gene expression in splenic tissues showed an increase in NF-kb, IL6, and TNF when animals were exposed to 400 mg/kg favipiravir. While these genes (NF-kb, IL6, and TNF) decreased when animals received a combination of favipiravir with dexamethasone. In gp3, hydropic degeneration was noted in both the kidney and liver. In Gp4, necrotic changes in the liver, and vacuolation of the renal glomerular tufts were observed. In Gp5, the necrotic hepatic tissues were infiltrated with mononuclear cells, and necrosis and inflammation in renal tubules in the kidney were shown. In gp6, leukocytic infiltration was noted in both the kidney and liver. In conclusion, the anti-Covid-19 drugs could induce pathological changes in the internal organs of the rat.

KEYWORDS

COVID-19, Favipiravir, Dexamethasone, Histopathology

INTRODUCTION

In Wuhan, Hubei province, China there was a spreading of an unknown disease-caused respiratory disorder at the end of December 2019. The causative agent of this pandemic pneumonia was identified as a novel coronavirus (nCoV), named severe acute respiratory syndrome coronavirus 2 (SARS-CoV-2) and also named by World Health Organization (COVID-19) considering it a pandemic virus as it spreads from China to all over the world (Ciotti *et al.*, 2020; He *et al.*, 2020).

Coronaviruses are single-strand RNA, positive sense, and enveloped virus contain 4 structural proteins include (nucleocapsid (N), membrane (M), envelope (E) and spike (S) proteins), these spikes protruded from its surface (Yuki *et al.*, 2020; Li *et al.*, 2020).

Angiotensin converting enzyme 2 (ACE2) was identified as an important receptor for SARS-CoV2. ACE2 is ubiquitously expressed in the respiratory system and other organs of the human body such as kidneys, bladder, heart, and ileum. Attachment and fusion of the virus to the host cell is mediated via the viral spikes' subunits S1 and S2 respectively. Once introduced inside the host cell, the viral RNA is replicated and new viral particles are manufactured and released outside the cell (Yuki *et al.*, 2020).

Favipiravir is an antiviral drug which had great effect on the treatment of COVID-19 patients, and corticosteroids drugs such as dexamethasone are also noted in the treatment protocol of

corona virus (Tarighi *et al.*, 2021).

Favipiravir (t705) commercially known as Avigan is manufactured by Toyama chemical Co., Ltd located in Tokyo, Japan. Favipiravir is as a purine acid base analog. It functions as an antiviral agent via inhibition of the RNA dependent RNA polymerase enzyme in RNA viruses. Favipiravir is a prodrug that gets converted to its active form, favipiravir ribofuranosyl-5'-triphosphate (favipiravir-RTP) through intracellular phosphoribosylation. This favipiravir-RTP acts as a sub-strand for RNA viruses as it determines RNA dependent RNA polymerase (RdRp) of virus and inhibits it by an integration process of drug into the viral RNA strand leading to viral mutation, termination of viral chain, prevention of chain extension, and inhibiting viral activity through halting viral transcription, replication and viral protein synthesis (Baranovich *et al.* 2013; Samson *et al.*, 2021).

On a kidney biopsy performed on a 16 years old girl treated for COVID-19 with favipiravir, there was extensive widespread glomerular damage represented by circumferential crescents formation, increased mesangial matrix, prominent endocapillary proliferation, glomerular necrosis and neutrophilic infiltrations sometimes with fibrin and hemorrhage. The renal tubules were degenerated with desquamation of epithelial cells and the interstitium was edematous and infiltrated with mononuclear inflammatory cells (Tastemel Ozturk *et al.*, 2021).

In a toxicologic study of favipiravir effect on a rat model, it

was found to induce deleterious effects on the liver and kidneys. The liver showed necrosis of hepatocytes, deposition of collagen, congestion of blood vessels, and dilated sinusoids. The kidneys showed tubular necrosis, deposition of collagen, loss of brush border, and dilation of the lumen of renal tubules. These lesions were recorded in different degrees from moderate to severe (Kara et al., 2023).

A percutaneous biopsy from the liver of woman who received favipiravir tablets for 2 weeks showed a hepatocellular cholestasis with bilirubinostasis and inflammatory cells in the portal tracts that consist of lymphocytes mixed with eosinophils (Kumar et al., 2021). In another study investigating the effect of favipiravir on the reproductive function in female rats, it was found to induce follicular cell degeneration and necrosis with cortical fibrosis (Bilici et al., 2023). The aim of this study was to investigate the pathologic, biochemical and molecular effects induced by the anti-COVID-19 drug favipiravir in a rat model when administered alone or together with dexamethasone.

MATERIALS AND METHODS

Drugs

Favipiravir: Present in film coated tablets, each tablet contains 200 mg and purchased from EVA Pharma for Pharmaceuticals & Medical Appliances Company.

Dexamethasone: Tablet contains 0.5 mg from Kahira Pharmaceuticals and chemical industries company.

Experimental animals

30 rats weighing at the beginning of the experiment 200 ± 10 g were obtained from the animal house, Faculty of Veterinary Medicine, Zagazig University (Zagazig, Egypt). Each 5 rats were housed in a cage at $25 \pm 0.5^\circ\text{C}$ under 12:12 light / dark cycle with free access of feed and water. Rats of all groups were kept under similar environmental conditions. Rats were acclimatized for 2 weeks before onset of the experiment. This study received an ethical approval number of ZU-IACUC/2/F/284/2023.

Experimental design

Experimental groups

A thirty mature albino rats were divided randomly into 6 groups; each group contained 5 rats. Group 1 was kept as a control with a free access to feed and water (negative control), Group

2 received 0.54 mg/kg of dexamethasone, Group 3 received 200 mg/kg of favipiravir (kara et al., 2023; Atçali et al., 2022), Group 4 received 400 mg /kg of favipiravir (Balci et al., 2022; Bilici et al., 2023), Group 5 was administered 200 mg/kg of favipiravir and 0.54 mg/k of dexamethasone, Group 6 received 400 mg/kg of favipiravir and 0.54 mg/kg of dexamethasone. All groups were sacrificed on the 8th day (Table 1).

Sample and tissue collection

Blood samples were collected from the medial canthus of the eye under anesthesia and put into blood collection tubes, that was allowed to stand for half an hour until blood clotted, left in the refrigerator for retraction of clot for 4 h, centrifuged to separate the serum and finally stored at -20°C to be used for estimation of various biochemical variables. Parts of liver and kidney tissues were rinsed with ice-cold phosphate-buffered saline (PBS), and dried between two filter papers, for estimation of MDA and TAC antioxidant parameters. Portion of the spleen was collected for gene expression and preserved at -80°C . Specimens from the liver, kidney and lung were collected and fixed in 10% neutral buffered formalin for histopathological studies.

Gene expression analysis

The real-time Polymerase Chain Reaction protocol was done according to the method previously described (Siniscalco et al., 2011). Briefly, total RNA was extracted from 25 mg of spleen tissue using Trizol (Invitrogen; Thermo Fisher Scientific, Inc.) (Livak and Schmittgen, 2001).

Histopathological specimens

The formalin-fixed liver, kidney and lung specimens were dehydrated in ascending grades of alcohol (70–100%), cleared in xylene, and embedded in paraffin wax. About 4-5 μm - thick paraffin sections were cut and stained with H&E (hematoxylin and eosin) and then examined and photomicrographed using a digital camera attached to a compound light microscope (Survarna et al., 2018).

Statistical analysis

All the numerical data were collected and tested for normality by the Anderson-Darling test. Statistical analysis was done, using SPSS software (version 16.0; Chicago, USA). The data were expressed as mean \pm standard error (SEM). The One-Way ANOVA

Table 1. Animal groups and numbers, drug doses and scarification.

Group	Drug/Agent	Dose (mg/kg B.W.)	Route	Frequency	Duration	Euthanasia
Group 1	Saline	10	Oral administration	Daily	7 days	After 8 days
Group 2	Dexamethasone	0.54	Oral administration	Daily	7 days	After 8 days
Group 3	Favipiravir	200	Oral administration	Daily	7 days	After 8 days
Group 4	Favipiravir	400	Oral administration	Daily	7 days	After 8 days
Group 5	Favipiravir + dexamethasone	200 + 0.54	Oral administration	Daily	7 days	After 8 days
Group 6	Favipiravir + dexamethasone	400 +0.54	Oral administration	Daily	7 days	After 8 days

Table 2. Primers used in PCR.

	Forward primer (5'-3')	Reverse primer (5'-3')	Size	Accession no.
IL6	ATATGTTCTCAGGGAGATCTTGGAA	GTGCATCATCGCTGTTTCATACA	80 NM	12589.2
NF kB	CAGGACCAGGAACAGTTCGAA	CCAGGTTCTGGAAGCTATGGAT	150NM	199267.2
TNF- α	AGGGTCTGGGCCATAGAAC	CCACCACGCTCTTCTGTCTAC	103 NM	12675.3

followed by post hoc "Duncan's test" was done to reveal the significant differences between AST, ALT, Urea, Creatinine and CRP, in all groups respectively. Also, for the evaluation of gene expression (IL6, NF-KB and TNF). While the student t test (independent t- test) for revealing the significant differences between both of TAC (ng/min/g tissue) and MDA (nmol/g tissue) in the liver and kidney tissues in the previously mentioned groups.

RESULTS

Serum biochemical analysis

The level of both AST and ALT showed a highly significant increases in group 6 followed by group 4, then group 5 and begins to decrease in group 3 followed by the control group. The level of urea is significantly increased in group 6 followed by group 4 and was moderate in group 5, then significantly decreased in group 3 followed by the control. The level of creatinine is signifi-

cantly increased in group 6 followed by group 4 and moderately increased in group 5 then group 3. The CRP level was significantly increased in group 4 then group 6, 5, and 3, respectively. The level of TAC in both liver and kidney tissues is significantly decreased in the treatment groups compared to the control. The level of MDA in both liver and kidney tissues is significantly increased in group 6 followed by 4, and finally 5 (Figs. 1-3).

Gene expression

The level of NF-Kb/gapdh was significantly increased in group 4 followed by group 3 then it was declined in the other groups until reaching to the normal range as in the control saline group. There are no significant differences between the level of both IL-6/gapdh and TNF-a/gapdh. They were significantly increased in group 4 followed by group 5 and 3 respectively, in relation to the control saline group (Fig. 4).

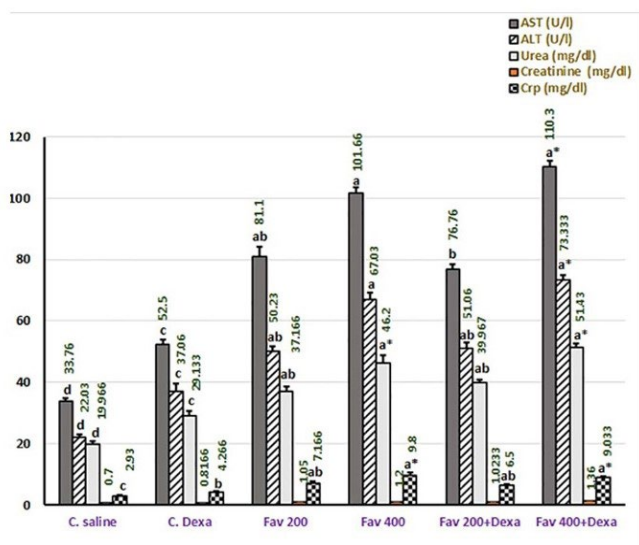


Fig. 1. AST, ALT, Urea, Creatinine and CRP in the experimental groups. Columns with the same color and carrying different letter (a*, a, ab, b, bc, c and d) are significantly different. The data are expressed as the Mean \pm SEM; differences are considered significant at $p \leq 0.05$ (one way ANOVA test followed by the post Hoc Duncan test).

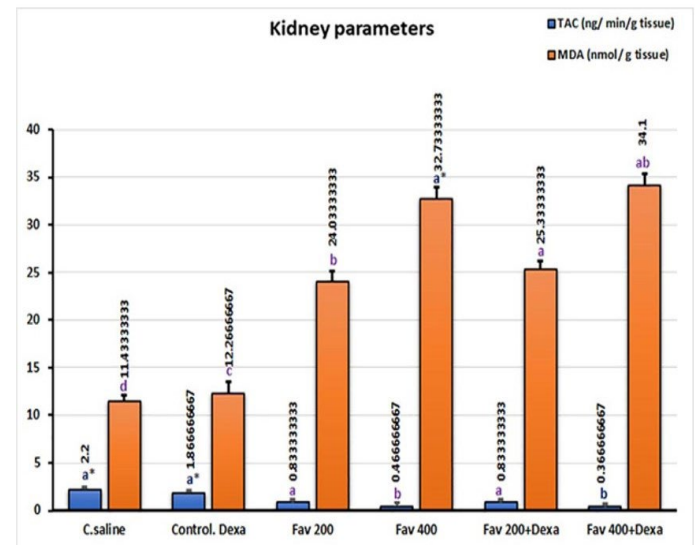


Fig. 3. TAC and MDA levels in the kidney tissues of the experimental groups. Columns with the same color and carrying different letter (a*, a, ab, b, bc, c and d) are significantly different. The data are expressed as the Mean \pm SEM; differences are considered significant at $p \leq 0.05$ (one way ANOVA test followed by the post Hoc Duncan test).

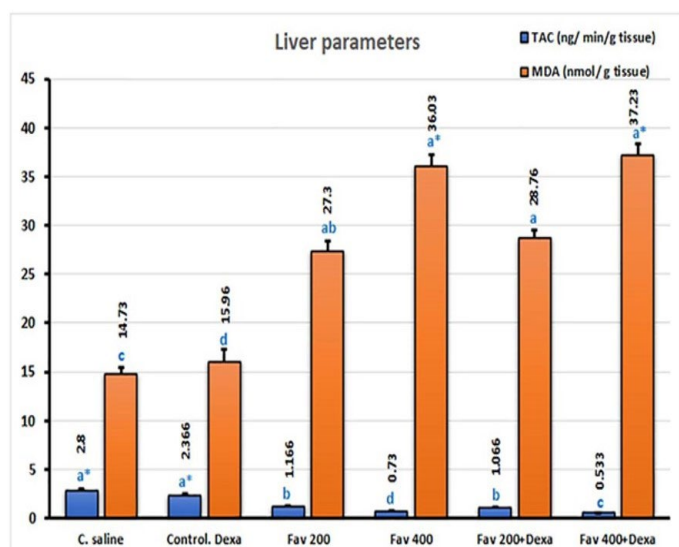


Fig. 2. TAC and MDA levels in the liver tissues of the experimental groups. Columns with the same color and carrying different letter (a*, a, ab, b, bc, c and d) are significantly different. The data are expressed as the Mean \pm SEM; differences are considered significant at $p \leq 0.05$ (one way ANOVA test followed by the post Hoc Duncan test).

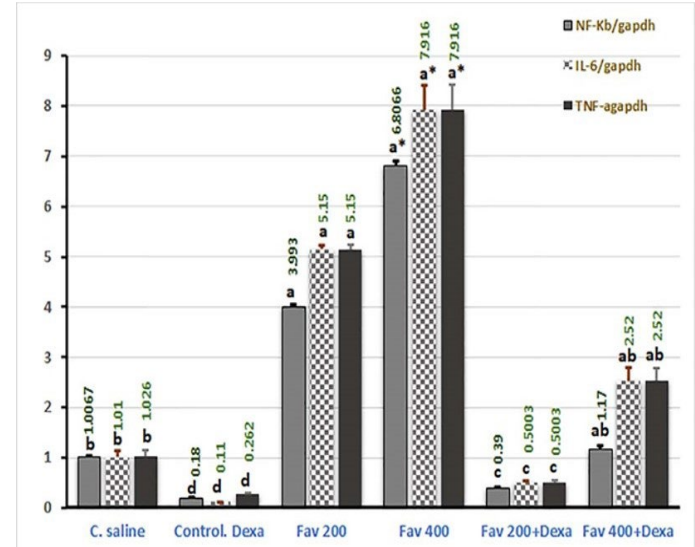


Fig. 4. Gene expression of NF-Kb/gapdh, IL-6/gapdh and TNF-a/gapdh in all treatment groups. Columns with the same color and carrying different letter (a*, a, ab, b, bc, c and d) are significantly different. The data are expressed as the Mean \pm SEM; differences are considered significant at $p \leq 0.05$ (one way ANOVA test followed by the post Hoc Duncan test).

Histopathological examination

GP1 (control) showed normal histological structure of liver, kidneys and lungs.

In Gp2 where rats received 0.54 mg/kg dexamethasone, kidneys showed thickening and hyalinization in the wall of renal blood vessel with hydropic degeneration in the epithelial cells. While the liver showed dilated central vein and portal vein with individualization of hepatocytes. The lungs showed mild thickening in the inter alveolar septa by mononuclear cells.

Gp3 in which rats received 200 mg/kg favipiravir, showed congestion of peritubular capillaries and vacuolation of endothelial cells of glomerular tufts in the kidneys (Fig. 5a), together with hydropic degeneration in epithelial cells of the renal tubules (Fig. 5b), in addition to necrosis in epithelial cell in renal tubules with pyknotic nuclei (Fig. 5c). The liver showed congestion of central vein with perivascular round cells infiltration (Fig. 5d). acute cell swelling as well as fatty change in some hepatocyte (Fig. 5e). The portal area showed congestion of portal vein with mild aggregation of mononuclear cells and hyperplasia in Kupffer cells were seen (Fig. 5f). Some degenerative changes in hepatocytes represented by vacuolar and hydropic degeneration were seen as well(Fig. 5g). The lungs showed catarrhal bronchitis represented by desquamation of epithelial cells inside the lumen of bronchus with leukocytic infiltration in the lamina propria, and thickening of inter alveolar septa by RBS, hemosiderin and mononuclear cells and eosinophils, as well as peribronchial eosinophilic cells aggregation had been detected. (Fig 5h and i)

In Gp4 where rats received 400 mg/kg favipiravir, the kidneys showed vacuolation in glomeruli tufts and the epithelial cells of some renal tubules showed mild vacuolation. The lumen of few renal tubules showed epithelial casts (Fig. 6a). In the liver, congestion of hepatic sinusoid was evident and the portal areas showed congestion of portal vein with mild thickening of bile duct wall by mononuclear cells infiltraton and newly formed bile ductules were seen (Fig. 6b and c) the hepatocytes showed some degenerative change with presence of apoptotic bodies (Fig. 6d).

The lungs showed catarrhal bronchitis and thickening of inter alveolar septa with mononuclear cells and rbcs with some alveoli showing atelectasis and other showing emphysema (Fig. 6e), in addition to thickening and hyalinization in the wall of blood vessels with perivascular aggregation of mononuclear cells (Fig. 6f),

In Gp5, where rats received 200 mg/kg favipiravir + 0.54 mg/kg dexamethasone, the kidney's glomeruli showed vacuolation and congestion of glomeruli tufts. some necrotic and inflammatory changes were detected in renal tubules with complete degeneration of the epithelial cell of renal tubules in addition to infiltration of some leukocytes (Fig. 7a). Moreover, thickening and hyalinization in the wall of renal blood vessel with perivascular edema (Fig. 7b) were noted. In the liver sections, hepatocytes showed some degenerative changes represented by fatty change (Fig. 7c) with presence of focal necrotic area infiltrated with mononuclear cell (Fig. 7d). Vacuolar and hydropic degeneration were seen in hepatocytes (Fig. 7e). In the examined pulmonary sections some alveoli were filled with faint eosinophilic fibrin threads with proliferation of pneumocyte type 2 and leukocytic infiltration (Fig. 7f). Thickening of interalveolar septa with mononuclear cell infiltration, as well as emphysema and atelectasis were observed.

Finally, in GP6 were rats received 400 mg/kg favipiravir + 0.54 mg/kg dexamethasone, kidneys showed necrotic changes in epithelial cells of renal tubules (Fig. 8a) represented by complete disappearance of nuclei in addition to leukocytic infiltration in between the affected renal tubules and hemorrhage between renal tubules (Fig. 8b) were seen. In the liver sections, some hepatocytes showed vacuolation with pyknosis of the nucleus (Fig. 8 c) and the portal areas showed proliferated bile ducts with leukocytic infiltrations and individualization of fewer hepatocyte (Fig. 8d). Proliferation of Kupffer cells were also noted. The lungs showed thickening in interalveolar septa with RBCs, mononuclear cell and brown pigment of hemosiderin (Fig. 8e). Focal area of suppurative inflammation with presence of giant cell and emphysema (Fig. 8f) were observed as well.

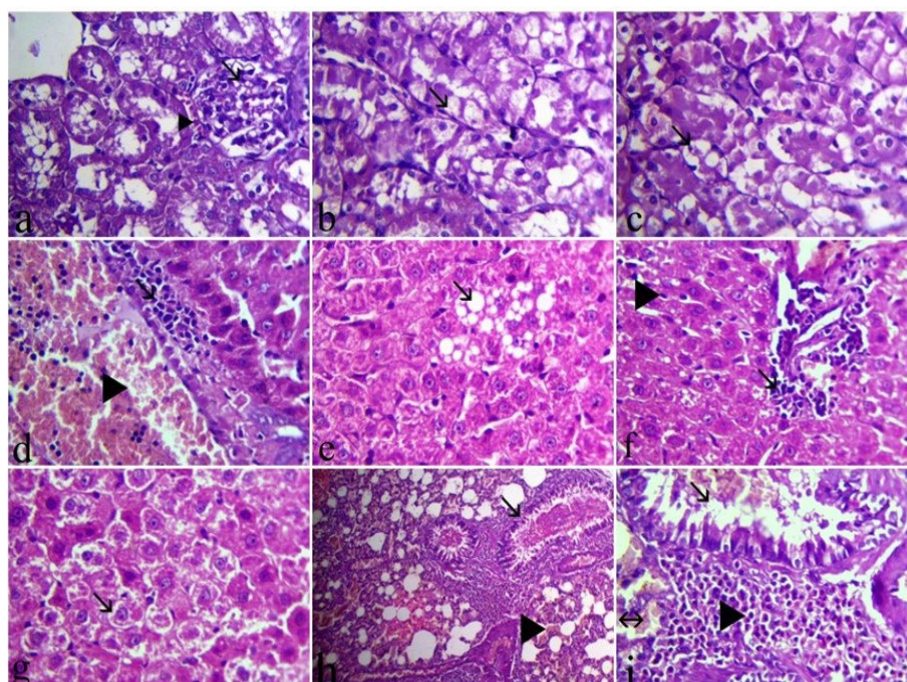


Fig. 5. Photomicrograph of H&E (GP3) stained kidney (a-c): a- vacuolation of glomeruli (arrow) congestion of peritubular capillary (arrowhead) X1200. b: hydropic degeneration (arrow), c: necrosis in renal tubules (arrow) x1200. The liver (d-g), d: congestion of central vein (arrowhead) mononuclear cells infiltration (arrow), e: fatty change (arrow) x1200. f: hyperplasia in kuffer cell (arrowhead) leukocytic infiltration (arrow) g: hydropic degeneration (arrow) x1200. The lung (h-i), h: catarrhal bronchitis (arrow) thickening of interalveolar septa with rbcs (arrowhead) x300. i: high power of previous figure (h) to show desquamated epithelial cell (arrow), peribronchial eosinophilic infiltration (arrowhead) thickening of interalveolar septa with rbcs (arrow with 2 head) x1200.

DISCUSSION

Favipiravir is one of the broad spectrum antiviral drugs that act as RNA polymerase inhibitors, it proved its activity against a large number of RNA viruses in addition to pandemic COVID 19. Almost all studies on favipiravir indicated that favipiravir had toxicological side effects on different organs specially kidney and liver (Kara et al., 2023).

Our work aimed to detect the side effects of favipiravir as antiviral drug and favipiravir with dexamethasone for treating COVID 19, through studying the pathological changes in the tissues of Albino rats. Besides, clinicopathological alterations of serum biochemical parameters and alteration in genes expression of some proinflammatory and immune markers were investigated in the spleen.

Our results in the kidney of rats in group 3 agreed partially

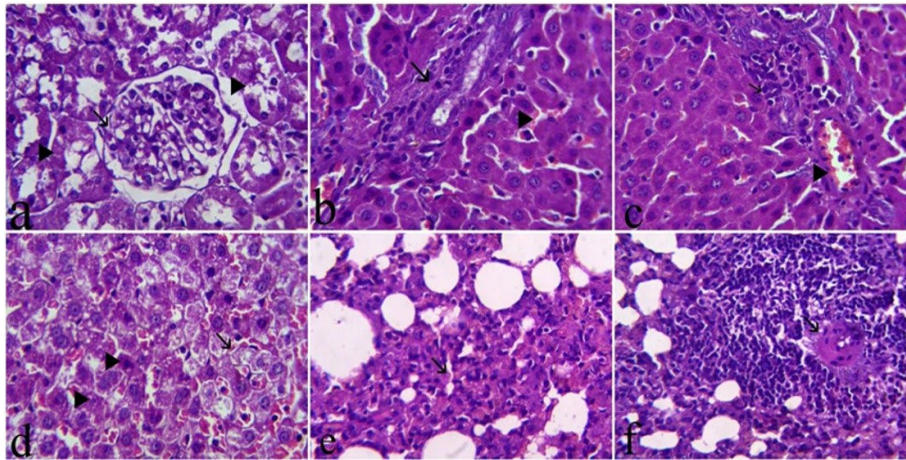


Fig. 6. Photomicrograph of H&E (Gp4) stained kidney (a): a- vacuolation of glomeruli (arrow) mild vacuole in renal epithelium (arrow head) X1200 liver (b-d) b: congestion of hepatic sinusoids (arrow head) mild thickening of bile duct (arrow) x1200. C-congestion of portal vein (arrowhead), focal aggregation of mononuclear cells in portal area (arrow) x1200. d: congestion of hepatic sinusoids (arrow), apoptotic body (arrowhead) x1200. (e-f)lung: e thickening of interalveolar septa by mononuclear cells (arrow). F: focal aggregation of mononuclear cells (arrow)x1200.

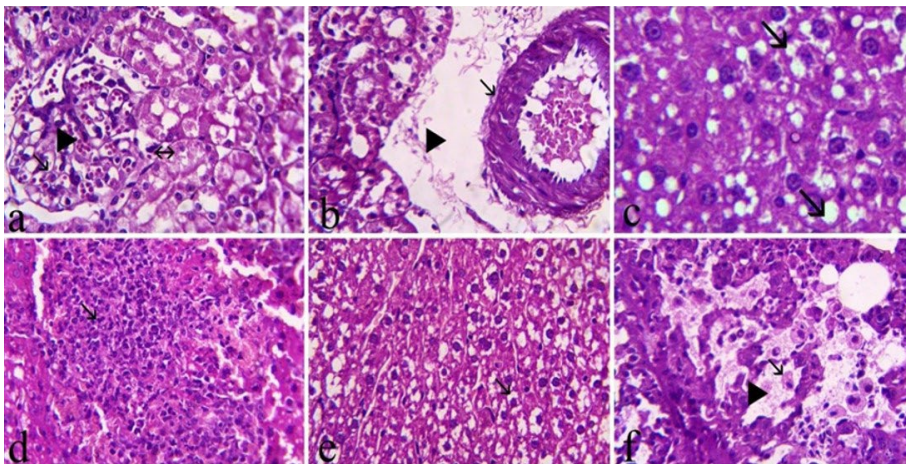


Fig. 7. Photomicrograph of H&E (GP5) stained kidney. (a-b): a- complete degeneration in the epithelial cell of renal tubules (arrow with 2 head) vacuolation of glomeruli (arrow) hemorrhage (arrowhead) X1200. b: Perivascular edema (arrowhead) thickening of renal blood vessel (arrow) X1200. Liver (c-e), c fatty change (arrow) x1200. d: focal necrotic area infiltrated with mononuclear cell (arrow) x1200. e: hydropic degeneration (arrow) x 1200. Lung (f) alveoli show fibrin threads (arrow head) with pneumocyte type 2 (arrow) x 1200.

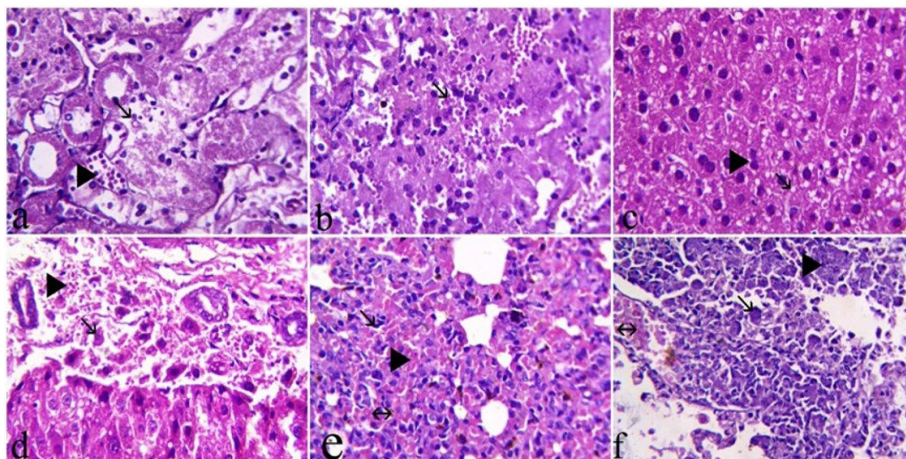


Fig. 8. Photomicrograph of H&E (GP6) stained kidney (a-b): a showed necrotic change in epithelial cells lining renal tubules (arrow) congestion of peritubular capillary (arrowhead) X1200.b: hemorrhage between renal tubule (arrow) x1200. The liver (c-d) c: liver showed vacuole (arrow) pyknotic nuclei (arrowhead) x 1200. d: Individualization of hepatocyte (arrow) hemorrhage (arrowhead) x 1200. the lung (e-f) e: thickening of interalveolar septa by Mononuclear cells (arrow) Brown pigment of hemosiderin (arrow with 2 head) RBCs (arrowhead) x 1200. f: Suppurative inflammation (arrowhead) giant Cell (arrow) Thickening in inter alveolar Speta with hemorrhage (arrow with 2 head) x 1200.

with (Tastemel Ozturk *et al.*, 2021) who observed necrosis, hydropic degeneration and hemorrhage in the kidney of human after taking FAV, as he observed karyorrhexis, proliferation of endocapillaries, increase in mesangial matrix and presence of fibrin in the most of glomeruli.

The results of the kidney of rats in group 5 and 6 are partially in agreement with the results of Tastemel Ozturk *et al.* (2021) who observed necrotic changes, leukocytic infiltration and edema, thickening of renal blood vessels in kidney of human after taking favipiravir where we observed complete degeneration in the epithelial cell of renal tubules, perivascular edema and complete disappearance of nuclei.

Our results in the liver of the rats in group 4, agreed with Kara *et al.* (2023) who observed hepatic necrotic and congestion of portal vein and hepatic sinusoid in liver of rats after taking FAV (200 mg/kg for 10 days) where he observed deposition of the collagen. Besides, Kumar *et al.* (2021) observed congestion and inflammation in portal tracts in liver of the human after taking favipiravir for 2 weeks where he observed hepatocellular cholestasis with bilirubinostasis. Results of the lung of rats in group 3, and 4 are in a partial agreement with Akbal-Dagistan *et al.* (2022) who observed infiltration of the inflammatory cells, inflammation in bronchial lumen in the lung of rat after taking FAV by inhalation, on the other hand, we observed catarrhal bronchitis, desquamation of epithelial cells, some alveoli showing atelectasis and other showing emphysema.

Regarding liver function tests, the results of the present study agreed with Kaur *et al.* (2020) and Yamazaki *et al.* (2021) who observed that administration of favipiravir to human lead to elevated ALT and AST activities. Besides, Kara *et al.* (2023) observed that favipiravir in albino rats lead to elevated AST, ALT, Urea, creatinine and CRP and also favipiravir lead to increased MDA in liver and kidney tissues.

The results of the proinflammatory cytokines were in agreement with the results of Doğan *et al.* (2023) who observed that favipiravir lead to elevated proinflammatory cytokines (TNF- α and IL-6) in liver and kidney of rats. While Ozbas *et al.* (2021) reported a decrease in CRP of human. Akbal-Dagistan *et al.* (2022) reported that favipiravir did not change the levels of ALT, AST, creatinine and urea from normal range.

Our results are partially in agreement with Balci *et al.* (2022) who recorded that favipiravir at a high dose could increase MDA level in the different organs of the rat, particularly in the ovary. Renal and hepatic parameters can be affected by the concentration of favipiravir drug which can lead to impairment of the hepatic and renal cells (Marra *et al.*, 2021). The elevation in renal and hepatic parameters were concluded as favipiravir cause changes in pharmacokinetics effects that may lead to toxicity. (Kara *et al.*, 2023)

Increasing the dose of favipiravir lead to an increase in the toxicity of the tested drugs (Driouich *et al.*, 2021). Favipiravir is metabolized in the liver through aldehyde oxidase (AO) especially through xanthine oxidase. This process led to the creation of inactive oxidative product (hydroxylated) which also called (T-705M1) which is harmful for kidney and liver (Mishima *et al.*, 2020). In our opinion elevated liver and kidney functions, MDA and genes expression (IL6, TNF & NF-KB) are indicators for the lesions which were observed in liver, kidney and lung.

CONCLUSION

Favipiravir is partially safe antiviral drug, favipiravir with dexamethasone are not recommended and we recommend administration of some antioxidant drugs to reduce free radicals and elevate antioxidants in the body.

CONFLICT OF INTEREST

The authors declare that they have no conflict of interest.

REFERENCES

- Akbal-Dagistan, O., Sevim, M., Sen, L.S., Basarir, N.S., Culha, M., Erturk, A., Yildiz-Pekoz, A., 2022. Pulmonary delivery of favipiravir in rats reaches high local concentrations without causing oxidative lung injury or systemic side effects. *Pharmaceutics* 14, 2375.
- Atçali, T., Yakut, S., Çağlayan, C., Ulucan, A., Kara, A., 2022. Effects of favipiravir on hematologic parameters and bone marrow in the rats. *J. Exper. Clin. Med.* 39, 156-159.
- Balci, S., Çöllüoğlu, Ç., Yavuzer, B., Bulut, S., Altındağ, F., Akbaş, N., Süleyman, H., 2022. Effect of low and high dose of favipiravir on ovarian and reproductive function in female rats: Biochemical and histopathological evaluation. *Gen. Physiol. Biophys.* 41, 457-463.
- Baranovich, T., Wong, S.S., Armstrong, J., Marjuki, H., Webby, R.J., Webster, R.G., Govorkova, E.A., 2013. T-705 (favipiravir) induces lethal mutagenesis in influenza A H1N1 viruses in vitro. *J. Virol.* 87, 3741-3751.
- Bilici, S., Altuner, D., Suleyman, Z., Bulut, S., Sarigul, C., Gulaboglu, M., Suleyman, H., 2023. Favipiravir-induced inflammatory and hydropic degenerative liver injury in rats. *Advances in Clinical and Experimental Medicine: Official Organ Wroclaw Medical University.*
- Ciotti, M., Ciccozzi, M., Terrinoni, A., Jiang, W.C., Wang, C.B., Bernardini, S., 2020. The COVID-19 pandemic. *Crit. Critical Rev. Clin. Lab. Sci.* 57, 365-388.
- Doğan, M. F., Kaya, K., Demirel, H. H., Başeğmez, M., Şahin, Y., Çiftçi, O., 2023. The effect of vitamin C supplementation on favipiravir-induced oxidative stress and proinflammatory damage in livers and kidneys of rats. *Immunopharmacol. Immunotoxicol.* 14, 1-6.
- Driouich, J.S., Cochlin, M., Lingas, G., Moureau, G., Touret, F., Petit, P.R., Nougairède, A., 2021. Favipiravir antiviral efficacy against SARS-CoV-2 in a hamster model. *Nature Commun.* 12, 1735.
- He, F., Deng, Y., Li, W., 2020. Coronavirus disease 2019: What we know?. *J. Med. Virol.* 92, 719-725.
- Kara, A., Yakut, S., Çağlayan, C., Atçali, T., Ulucan, A., Kandemir, F.M., 2023. Evaluation of the toxicological effects of favipiravir (T-705) on liver and kidney in rats: biochemical and histopathological approach. *Drug Chem. Toxicol.* 46, 546-556.
- Kaur, R.J., Charan, J., Dutta, S., Sharma, P., Bhardwaj, P., Sharma, P., Misra, S., 2020. Favipiravir use in COVID-19: analysis of suspected adverse drug events reported in the WHO database. *Infect. Drug Resist.* 15, 4427-4438.
- Kumar, P., Kulkarni, A., Sharma, M., Rao, P.N., Reddy, D.N., 2021. Favipiravir-induced liver injury in patients with coronavirus disease 2019. *J. Clin. Transl. Hepatol.* 9, 276.
- Li, H., Liu, S.M., Yu, X.H., Tang, S.L., Tang, C.K., 2020. Coronavirus disease 2019 (COVID-19): current status and future perspectives. *International J. Antimicrob. Agents* 55, 105951.
- Livak, K.J., Schmittgen, T.D., 2001. Analysis of Relative Gene Expression Data Using Real-Time Quantitative PCR and the $2^{-\Delta\Delta CT}$ Method. *Methods* 25, 402-408.
- Marra, F., Smolders, E.J., El-Sherif, O., Boyle, A., Davidson, K., Sommerville, A.J., Back, D., 2021. Recommendations for dosing of repurposed COVID-19 medications in patients with renal and hepatic impairment. *Drugs* 21, 9-27.
- Ozbas, H.M., Kayan, T., Yakarisik, M., Dulger, A.C., Ayvaz, M.A., Aydin, M., 2021. Role of Favipiravir on the Hematologic parameters in patients with COVID-19 infection: Favipiravir Related Hematologic parameters. *Med. Sci. Discov.* 8, 577-580
- Samson, A.M., Pranith, P.L., Kumar, E.S., Prasobh, G.R., 2021. A review on the use of favipiravir in treatment of covid 19. *World J. Pharm. Res.* 10, 138-145.
- Siniscalco, D., Giordano, C., Galderisi, U., Luongo, L., De Novellis, V., Rossi, F., Maione, S., Huang, H., Andrews, R.J., Chen, L., Hongtianji, B., 2011. Integrative Neuroscience Long-lasting effects of human mesenchymal stem cell systemic administration on pain-like behaviors, cellular, and biomolecular modifications in neuropathic mice. *Front. Integr. Neurosci.* 5, 79.
- Tarighi, P., Eftekhari, S., Chizari, M., Sabernavaei, M., Jafari, D., Mirzabeigi, P., 2021. A review of potential suggested drugs for coronavirus disease (COVID-19) treatment. *Europ. J. Pharmacol.* 895, 173890.
- Tastemel Ozturk, T., Baltu, D., Kurt Sukur, E.D., Ozsurekci, Y., Gucer, S., Basaran, O., Topaloglu, R., 2021. Acute kidney injury in a patient with COVID-19: Questions. *Ped. Nephrol.* 36, 4109-4110.
- Yamazaki, S., Suzuki, T., Sayama, M., Nakada, T.A., Igari, H., Ishii, I., 2021. Suspected cholestatic liver injury induced by favipiravir in a patient with COVID-19. *J. Infect. Chemother.* 27, 390-392.
- Yuki, K., Fujiogi, M., Koutsogiannaki, S., 2020. COVID-19 pathophysiology: A review. *Clin. Immunol.* 215, 108427.